EFFECT OF WIND TUNNEL AIR VELOCITY ON VOC FLUX FROM STANDARD SOLUTIONS AND CAFO MANURE/WASTEWATER

D. B. Parker, E. A. Caraway, M. B. Rhoades, N. A. Cole, R. W. Todd, K. D. Casey

ABSTRACT. *Researchers and practitioners have used wind tunnels and flux chambers to quantify the flux of volatile organic compounds (VOCs), ammonia, and hydrogen sulfide and estimate emission factors from animal feeding operations (AFOs) without accounting for effects of air velocity or sweep air flow rate. Laboratory experiments were conducted using a small rectangular wind tunnel (30.5 cm length, 15.2 cm width, 5.1 cm height). The objectives of the research were to (1) quantify the effect of wind velocity on VOC flux rates, (2) compare and contrast a two-film model with different wind speed corrections, and (3) provide insight into methods for either selecting appropriate wind tunnel velocities or conducting post-sampling wind velocity corrections to simulate field emission rates. Fluxes were measured on standard solutions and on manure/wastewater from beef cattle and dairy AFOs. Volumetric air exchange rates were varied between 0.6 and 44 exchanges per minute, corresponding to calculated longitudinal air velocities of 0.003 to 0.23 m s^{-1}. Exhaust air was sampled using stainless steel sorbent tubes and analyzed for eleven volatile organic compounds comprised of seven volatile fatty acids (VFAs: acetic, propionic, isobutyric, butyric, isovaleric, valeric, and hexanoic) and four heavier molecular weight semivolatile organic compounds (sVOCs: phenol, p-cresol, indole, and skatole) using gas chromatography/mass spectrometry. Sulfur-containing VOCs were quantified using a portable total reduced sulfur meter. Flux rates for VOCs with small dimensionless Henry's law constants (i.e., those found at AFOs) increased with increasing air velocity. The two-film model with an experimentally derived reference gas-film transfer coefficient was found to reliably predict VOC flux at velocities between 0.003 and 0.23 m s^{-1}. However, the two-film model did not reliably predict VOC flux with other air velocity correction formulae, an indication that flux is a function of wind tunnel geometry and turbulence factors, and not just average air velocity or sweep air flow rate. These results corroborate other studies that show that air velocity is a major factor affecting VOC fluxes from AFOs, verifying that an air velocity correction factor is required for estimating accurate VOC emission factors using wind tunnels and flux chambers.*

Keywords. *Emission rates, Flux chamber, Gas chromatography, Henry's law constant, Indolic, Odor, Phenolic, Two-film model, Volatile fatty acids.*

Volatile organic compounds (VOCs) and volatile inorganic compounds (VICs) are emitted from wastewater treatment plants, food processing plants, landfills, and animal feeding operations (AFOs) (Kim et al., 2006). VOCs are produced from the degradation of amino acids and carbohydrates in the intestines of humans and animals (Mackie et al., 1998) and from incomplete anaerobic digestion (Mata-Alvarez et al., 2000). Sunesson et al. (2001) identified 70 VOCs from dairies in Sweden using sorbent tubes and gas chromatography/mass spectrometry (GC/MS), with *p*-cresol, 2-butanone, ethyl acetate, α-pinene, and Δ3-carene found at the highest concentrations. Filipy et al. (2006) identified 73 VOCs emitted from a dairy lagoon, whereas Rabaud et al. (2002, 2003) identified 35 VOCs emitted from California dairies. The number of VICs appear to be less numerous. Two of the primary VICs emitted from AFOs are ammonia (NH_3) and hydrogen sulfide (H_2S).

VOC emissions are an important aspect of air quality for two reasons: (1) many VOCs are malodorous (Rabaud et al., 2002, 2003; Parker et al., 2007; Wright et al., 2005) and (2) some VOCs are photochemically reactive and are precursors to the formation of ozone, a regulated air pollutant (Aquino et al., 2007; Carter, 1994). The U.S. Environmental Protection Agency (USEPA) has defined "reactive VOCs" as any compound of carbon that participates in atmospheric photochemical reactions and excludes the nonreactive compounds including carbon monoxide, carbon dioxide, methanes, and ethanes in 40 CFR 51.100s (USEPA, 1995a).

Submitted for review in March 2009 as manuscript number SE 7945; approved for publication by the Structures & Environment Division of ASABE in May 2010. Presented at the 2008 ASABE Annual Meeting as Paper No. 083897.

Mention of trade names or commercial products in this article is solely for the purpose of providing specific information and does not imply recommendation or endorsement by the USDA or the Texas A&M University System.

The authors are **David B. Parker, ASABE Member Engineer,** Supervisory Research Agricultural Engineer, USDA-ARS U.S. Meat Animal Research Center, Clay Center, Nebraska, and formerly Professor, West Texas A&M University, Canyon, Texas; **Edward A. Caraway,** Research Associate, and **Marty B. Rhoades, ASABE Member Engineer,** Research Fellow, Department of Agricultural Sciences, West Texas A&M University, Canyon, Texas; **N. Andy Cole,** Research Animal Scientist and Lead Scientist, and **Richard W. Todd,** Research Scientist, USDA-ARS Conservation and Production Research Laboratory, Bushland, Texas; and **Kenneth D. Casey, ASABE Member Engineer,** Agricultural Engineer, Texas AgriLife Research, Texas A&M University System, Amarillo, Texas. **Corresponding author:** David B. Parker, USDA-ARS U.S. Meat Animal Research Center, Clay Center, Nebraska 68933; phone: 402-762-4277; fax: 402-762-4273; e-mail: david.parker@ars.usda.gov.

The quantification of VOC emissions from AFOs is important not only for estimation of emission factors from a regulatory standpoint, but also to determine which sources emit VOCs so that best management practices can be developed for reducing emissions and odors. There are several approaches to estimating emission rates: (1) the mass balance approach where source concentrations are measured over time and the difference is used to determine losses to the atmosphere, (2) indirect methods where ambient concentrations are measured and source emission rates are back-calculated using dispersion models, and (3) direct methods where emission rates are measured directly from the source using a wind tunnel or flux chamber (Hudson and Ayoko, 2008a; Hudson et al., 2009; NAS, 2003). Each of these methods has advantages and disadvantages that depend on the particular project goals. The mass balance approach is often preferred, but instances are few, especially for VOC emissions from large-area sources, where the mass balance approach can be used in field conditions.

As part of ongoing research to quantify VOC emissions from AFOs, and in an attempt to increase the knowledge base concerning measurement of VOC emissions with wind tunnels and flux chambers, several laboratory experiments were conducted to evaluate how wind velocity affects flux rates of VOCs commonly found at beef cattle feedyards and dairies. The specific objectives were to (1) quantify the effect of wind velocity on VFA and sVOC emission rates, (2) compare and contrast a two-film model with different wind speed corrections, and (3) provide insight into methods for either selecting appropriate wind tunnel velocities or conducting post-sampling wind velocity corrections to simulate field emission rates.

Literature Review

There has been a long-standing debate about the appropriateness and accuracy of wind tunnels and flux chambers for quantifying emissions at AFOs and other area sources (Hudson et al., 2009; Hudson and Ayoka, 2008a, 2008b; Zhang et al., 2002; Lindberg et al., 2002; Rhoades et al., 2005; Cole et al., 2007; Fowler et al., 2001; Meisinger et al., 2001; Whitehead and Rastrick, 1991; Ryden and Lockyer, 1985; USEPA, 1982; Vlek and Stumpe, 1978; Kissel et al., 1977; Watkins et al., 1972). Hudson et al. (2009) recently compared odor emissions from a wind tunnel (University of New South Wales design) and a flux chamber (commonly called the U.S. EPA flux chamber as designed by Kienbusch, 1986) and reported that wind tunnel odor emission rates were 60 to 240 times higher than those in the U.S. EPA flux chamber.

Many scientists have recognized that wind velocity and air flow across soil and liquid surfaces affects the flux of ammonia and some VOCs (Liss and Slater, 1974; USEPA, 1982; Delos et al., 1984; Mills et al., 1985; Eklund, 1992; Wanninkhof, 1992; Bidleman and McConnell, 1995; Zahn et al., 1997; Zhang et al., 2002; Lindberg et al., 2002; Leyris et al., 2005; Hudson and Ayoko, 2008a; Hudson et al., 2009). When measuring ammonia emissions from simulated retention pond and feedlot surfaces, Cole et al. (2007) reported that emissions from a flux chamber operated at 0.5 exchanges per minute were less than 25% of that from an open surface. Vlek and Stumpe (1978) compared ammonia losses from ammonium carbonate solutions in the laboratory and field, and determined that an air flow rate of 7.6 exchanges per minute was required in the laboratory to simulate the same flux rate measured in open containers placed outdoors. Downwind of a slurry storage basin at an operating swine farm, Zahn et al. (1997) reported a positive correlation between VOC flux and wind speeds ranging from 0.2 to 9.4 m s^{-1}. Among others, Zahn et al. (1997) and USEPA (1982) have suggested that Henry's law constant could be a useful parameter for predicting the emission behavior of individual VOCs. There have been several approaches to estimate the mass transfer of VOCs, one of which is the two-film model that uses Henry's law constant to predict emission rates.

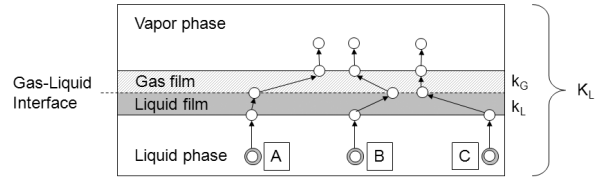

Figure 1. Conceptual diagram of the two-film model showing pathways for molecules that are gas-film controlled (A), liquid-film controlled (C), or both gas- and liquid-film controlled (B). The path length is indicative of the resistance to molecular movement (long path = high resistance).

The Two-Film Model

The conventional two-film volatilization model, once called the "stagnant-film model," has been used for describing volatilization of a solvent-solute mixture (Whitman, 1923; Lewis and Whitman, 1924; Liss and Slater, 1974; Sadek et al., 1996; Bianchi and Varney, 1997; USEPA, 1982). Much of the earlier research with the two-film model was related to estimating gas exchange over the ocean (Wanninkhof, 1992). The two-film model can be conceptually described by the diagram in figure 1.

As a VOC moves from the liquid phase to the vapor phase, it must pass through two films: the liquid film and the gas film. Some molecules pass with ease through one of the films, yet are impeded through the other film. If a VOC molecule is primarily gas-film controlled, then conceptually its path will follow that of molecule A in figure 1. If it is primarily liquid-film controlled, then it will follow the path of molecule C, and if a molecule is both gas- and liquid-film controlled, then it will follow the path of molecule B. Hudson and Ayoko (2008a) provide further discussion on this topic.

In the two-film model, the volatilization flux through these two films is defined as:

$$J = k_L\left(C_L - C_L^*\right) = k_G\left(C_G^* - C_G\right) \quad (1)$$

where J is the flux (mass/area-time), k_L is the liquid-film transfer coefficient (length/time), k_G is the gas-film transfer coefficient (length/time), C_L is the VOC concentration in the liquid phase (mass/volume), C_G is the VOC concentration in the vapor phase, C_L^* is the VOC concentration at the liquid film-gas film interface, and C_G^* is the VOC concentration at the gas film-vapor phase interface. Because C_L^* and C_G^* cannot be measured directly, equation 1 has been simplified assuming $C_G^* = H_{cc}\, C_L^*$ to obtain:

$$J = K_L\left(C_L - C_G/H_{cc}\right) \quad (2)$$

where K_L is the overall solute transfer coefficient, and H_{cc} is the dimensionless Henry's law constant discussed in more detail later. K_L is calculated using the equation:

$$K_L = \frac{k_L k_G H_{cc}}{k_L + k_G H_{cc}} \quad (3)$$

where k_L and k_G are the liquid-film and gas-film transfer coefficients, respectively.

If the VOC concentration in air (C_G) is low such that it does not inhibit the VOC flux, then equation 2 can be simplified to the following:

$$J = K_L\left(C_L - C_G/H_{cc}\right) \cong K_L\left(C_L\right) \quad (4)$$

Note that the equation 4 approximation is only valid when $C_G/H_{cc} << C_L$. At the other extreme, the flux will be zero (suppressed by the elevated gas concentration) when $C_G = C_L H_{cc}$, which will occur when air flow rates are very low.

Empirical correlations for estimating k_L and k_G have been proposed based on values for reference compounds, as summarized in Lee et al. (2004):

$$k_L = k_L^R\left(\frac{M_R}{M}\right)^{1/2} \quad (5)$$

$$k_G = k_G^R\left(\frac{M_R}{M}\right)^{1/2} \quad (6)$$

where k_L^R is the reference liquid-film transfer coefficient (i.e., oxygen), k_G^R is the reference gas-film transfer coefficient (i.e., water vapor), and M_R and M are the respective molecular weights of the reference substance (oxygen = 32 and water = 18) and the solute or VOC. The k_L^R of oxygen (0.2 m h^{-1}) and the k_G^R of water vapor (30 m h^{-1}) are often used for estimating k_L and k_G of the solute (Liss and Slater, 1974; Schwarzenbach et al., 2003; Lee et al., 2004).

Henry's Law Constants

Henry's law constants can be expressed in a variety of units as mass per volume per pressure (i.e., mg L^{-1} atm^{-1} or M atm^{-1}). Henry's law constant is often presented in its dimensionless form (H_{cc}) as:

$$H_{cc} = \frac{C_{air}}{C_{water}} \quad (7)$$

where C_{air} is the concentration in air (mass/volume), and C_{water} is the concentration in water (mass/volume) (Sawyer and McCarty, 1978; Buonicore and Davis, 1992). In this form, Henry's law states that, at equilibrium, the VOC concentration in the air is directly proportional to the VOC concentration in the water. Henry's law constants vary with temperature; thus, the VOC flux will vary with temperature. Sander (1999) presented the following formula for describing Henry's law as a function of temperature (T):

$$k_H = k_H^{\Theta} \exp\left(\frac{-\Delta_{so\ln}H}{R}\left(\frac{1}{T} - \frac{1}{T^{\Theta}}\right)\right) \quad (8)$$

where k_H is Henry's law constant (M atm^{-1}) at temperature T, k_H^{Θ} is Henry's law constant (M atm^{-1}) at standard conditions of T^{Θ} = 298.15 K, and $\frac{\Delta_{so\ln}H}{R}$ is the temperature dependence factor (K), which is also defined as $\frac{-d\ln k_H}{d\left(1/T\right)}$. The dimensionless Henry's law constant (i.e., eq. 7) is then calculated from k_H using:

$$H_{cc} = \frac{12.2}{k_H T} \quad (9)$$

Henry's law constants for several VOCs found at AFOs and industrial facilities are presented in graphical form in figure 2. Many of the Henry's constants were variable, covering one or two orders of magnitude. Most of the Henry's law constants in figure 2 are reported at or near standard temperature; nevertheless, there was some variability in reported temperatures, which explains some of the variation (Sander, 1999).

Methods of Incorporating Wind Velocity into the Two-Film Model

As summarized by Bianchi and Varney (1997), the early stagnant-film model (Liss and Slater, 1974) was recognized to significantly underestimate emission rates of some VOCs, primarily because of the failure to take into account wind velocity effects. Recognizing that wind velocity was a key element in VOC emission rates, several empirical methods were subsequently developed for incorporating wind velocity into the two-film model. Mills et al. (1985) and Delos et al. (1984) presented an equation for estimating k_G, which takes into account the effect of wind speed (V):

$$k_G = 170\left(\frac{18}{M}\right)^{1/4} V \quad (10)$$

where k_G is in m d^{-1}, and V is in m s^{-1}. Though the height of the wind speed is not always mentioned, most scientists have used either the 2 m or 10 m height (Wanninkhof, 1992).

Lee et al. (2004) introduced the "β concept" for calculating k_G, which includes an empirically determined turbulence factor based on the velocity in the wind tunnel:

$$k_G = \beta\left(\frac{RT}{2M_R\pi}\right)^{1/2} \quad (11)$$

where β is an empirical factor determined through laboratory experiments with a small wind tunnel that accounts for the efficiency of a vapor moving into air. Lee et al. (2004) reported that β was almost the same for different VOCs. A graph of Lee's β vs. air velocity (V) is shown in figure 3. Velocities were measured at a height of 4.5 cm above the water surface. Lee et al. (2004) found the sharpest increase in β between 0 and 0.2 m s^{-1}, which is within the range of velocities used in our current research.

The Importance of Henry's Law Constant and Wind Velocity on Emissions of AFO VOCs

In a project conducted at the U.S. EPA's Atmospheric Research and Exposure Assessment Laboratory, Gholson et al. (1989, 1991) evaluated the flux chamber method for measuring VOC emissions from quiescent liquid surfaces and stated that "varying the sweep flow rate was found to have little effect on the measured emission rate between 2 L/min and

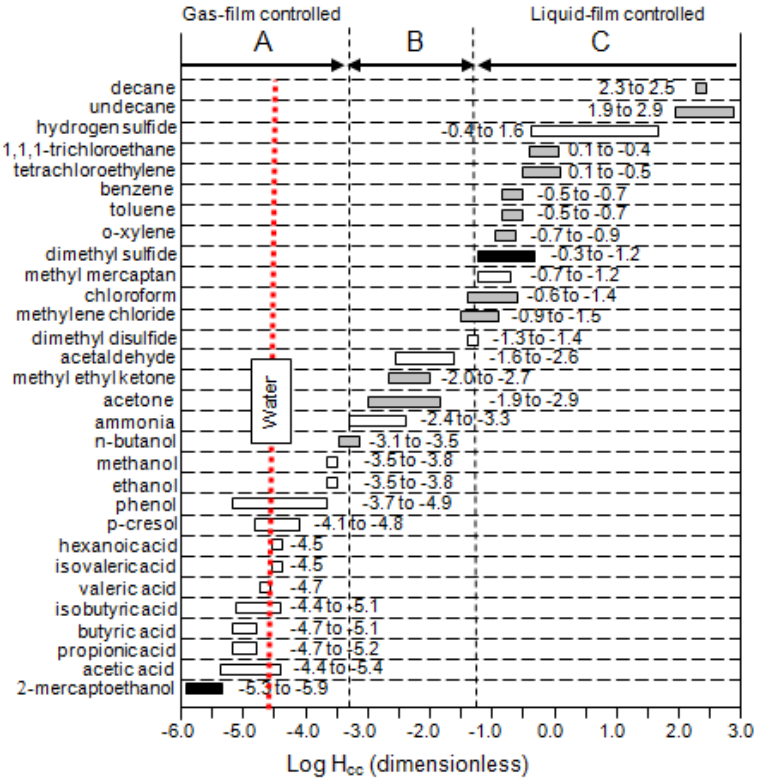

Figure 2. Representative ranges of dimensionless (log) Henry's law constants for VOCs and VICs. Open rectangles are compounds found at animal feeding operations in fresh manure, anaerobic treatment lagoons, or feed handling. Gray-shaded rectangles are compounds found primarily at industrial facilities. Black rectangles are sulfur-containing VOCs. The vertical dashed line is for water (logH_{CC} = -4.6). VOCs are either gas-film controlled (A), liquid-film controlled (C), or partially gas- and liquid-film controlled (B). This graph was adapted from Hudson and Ayoko (2008a). All ranges on Henry's law constants are from Sander (1999), with the exception of 2-mercaptoethanol, which is from IUCLID5 (2007).

10 L/min." This research has led some scientists to believe that flux chambers are appropriate for measuring all VOCs, including those at animal feeding operations. However, it is important to note that the VOCs that Gholson measured were those typically found in landfills and other industrial facilities. As shown in figure 2, industrial-type VOCs have much higher Henry's law constants (H_{cc}) than the VOCs typically found in animal feeding operations. With the exception of acetone and n-butanol, the industrial VOCs have H_{cc} values that make them liquid-film controlled as opposed to the VOCs at AFOs, which are gas-film controlled. When H_{cc} is greater than 1.0×10^{-3}, the VOCs are liquid-film controlled, and VOCs that are liquid-film controlled are not affected by wind velocity (Lee et al., 2004; Schwarzenbach et al., 2003; Liss and Slater, 1974; Hudson and Ayoka, 2008a). Thus, while Gholson's conclusion was appropriate for the VOCs that he measured, his conclusions were not valid for most VOCs found at CAFOs (fig. 2).

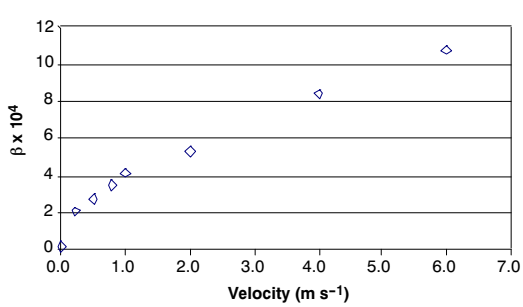

Figure 3. Relationship between β (eq. 11) and air velocity (Lee et al., 2004) with an air velocity measured at 4.5 cm above the water surface.

To demonstrate the importance of Henry's law constants and wind velocity effects, the two-film model with the Mills et al. (1985) velocity correction (eq. 10) was used to calculate and compare emission rates for typical VOCs found at AFOs (such as acetic acid and phenol) with those found at industrial and landfill facilities (such as 1,1,1-trichlorethane and tetrachloroethylene). To show the hypothetical effect on a single graph, in the model simulations the initial concentrations in water were set to 400 mg L^{-1} for acetic acid and phenol, and 10 mg L^{-1} for 1,1,1-trichlorethane and tetrachloroethylene. Wind velocities were varied from 0.1 to 2.0 m s^{-1}. As shown in figure 4, the two-film model with the Mills et al. (1985) correction factor predicts that wind velocity has a great effect on emissions of compounds with small H_{cc}, such as acetic acid and phenol, whereas wind velocity has little effect on emissions of compounds with large H_{cc}, such as 1,1,1-trichlorethane and tetrachloro–ethylene.

Materials and Methods

Wind Tunnel Design

Traditional wind tunnels are designed for uniformity of air flow both longitudinally and transversely. With typical wind velocities of 0.5 to 2.0 m s^{-1}, corresponding exchange rates of 30 to 120 exchanges per minute are achieved for a 1 m long test section. The wind tunnel in this research was designed

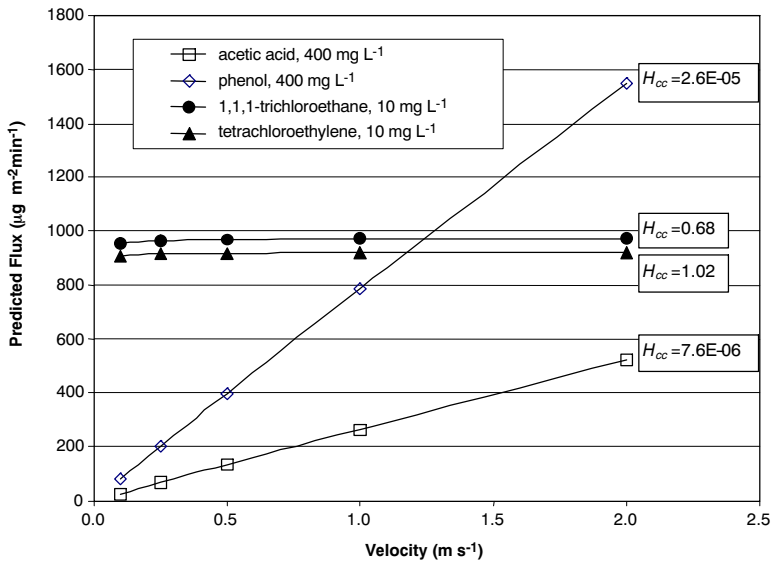

Figure 4. Flux rates predicted using the two-film model with Mills et al. (1985) velocity correction (eq. 10) demonstrating the effect of wind velocity at 2 m height on VOCs with differing Henry's law constants (H_{cc}).

and operated to simulate some operational aspects of the dome-shaped chamber type often referred to as the U.S. EPA flux chamber (Kienbusch, 1986; Gholsen et al., 1991; Eklund, 1992). For example, in the EPA flux chamber, air is distributed through small, equally spaced holes at low air flow rates (a flow rate of 5 L min^{-1} is often used, equivalent to a volumetric exchange rate of approximately 0.167 exchanges per minute). The low air flow rate of 5 L min^{-1} combined with the dome-shape make measurement or calculation of internal air velocities difficult because of the extremely low velocities, less than 0.05 m s^{-1} (Hudson and Ayoko, 2009; Hudson, 2009). Hudson (2009) had to increase the flow rate in the EPA chamber to 12 L min^{-1} in order to measure velocities above 0.05 m s^{-1} with a hot-wire anemometer.

The rectangular-shaped wind tunnel designed for this research provides for the ability to calculate longitudinal wind velocities, which cannot be done in dome-shape flux chambers such as the EPA-type flux chamber. The wind tunnel had dimensions of 5.1 cm height, 30.5 cm length, and 15.2 cm width (fig. 5), with a surface area of 0.046 m^2 and cross-sectional area of 0.0062 m^2 (based on an operating height of 4.1 cm allowing for 1 cm inset into the water or other media). The wind tunnel was constructed of 5 cm square steel tubing and 4.4 × 4.4 cm angle iron with a 5 mm thick Plexiglas top. Sweep air was dispersed into the wind tunnel through six 5 mm diameter holes equally spaced in the steel tubing at a height 2 cm above the emitting surface (fig. 5). Air exited the tunnel through three 1.3 cm diameter holes in the Plexiglas top at the opposite end of the tunnel.

Manure or liquid samples were placed in a shallow pan (32 × 18 cm) to a depth of 1 cm, and the wind tunnel was placed over the pan. The sweep air was supplied from a laboratory air compressor located in the temperature-controlled basement of an adjacent building. The relative humidity of the sweep air and the ambient temperature within the laboratory were measured occasionally throughout the experiments (VWR model 61161 humidity/temperature meter). The sweep air RH was consistently 21% throughout the experiments, and the ambient laboratory temperature ranged from 21°C to 22°C.

The sweep air was passed through an activated carbon filter to remove any VOCs in the compressed air, and then through a rotameter and into the wind tunnel. Carbon-filtered air was confirmed to be VOC-free via GC/MS analyses. The sweep air flow rate was controlled using one of three valved rotameters selected for low, medium, or high flow rates, respectively: Cole Parmer N102-05, 0 to 3.9 L min^{-1} (±0.1 L min^{-1}, ±2.6% of full range, ±9.1% of lowest flow rate of 1.1 L min^{-1}); Gilmont GF-6541-1230, 0 to 25 L min^{-1} (±1 L min^{-1}, ±4.0% of full range); and Gilmont 127 mm, 0 to 500 L min^{-1} (±5 L min^{-1}, ±1.0% of full range, ±5.9% of highest flow rate of 85 L min^{-1}).

The rotameters were calibrated by the manufacturers, and calibration certificates were provided. In the experiments, sweep air flow rates ranged from 1.1 to 85 L min^{-1}, corresponding to sweep air volumetric exchange rates of 0.6 to 44 exchanges per minute. Calculated average internal

Figure 5. Photograph of the small wind tunnel used in the research. Air entered the wind tunnel through the small holes in the upper right, and exited through the holes at the lower left.

longitudinal air velocities ranged from 0.003 to 0.23 m s^{-1}. These calculated velocities assume a uniform air distribution across the width and height of the wind tunnel cross-section. Turbulence and thus an increase in effective vertical velocities would increase with increasing air flow.

Calculated air velocities leaving the small 5 mm diameter holes ranged from 0.156 m s^{-1} at the lowest sweep air flow rate of 1.1 L min^{-1}, to 12.0 m s^{-1} at the highest sweep air flow rate of 85 L min^{-1}. This compares to air velocities of 0.29 m s^{-1} leaving the holes for a sweep air flow rate of 5 L min^{-1} in the U.S. EPA flux chamber (Eklund, 1992). At this flow rate, the wind speed in the U.S. EPA flux chamber has been described as "still, but not stagnant" (Eklund, 1992). The wind tunnel designed for this research had air velocities leaving the holes that encompassed that of the U.S. EPA flux chamber (0.156 to 12.0 m s^{-1} as compared to 0.29 m s^{-1}), and overall sweep air exchange rates greater than that of the U.S. EPA flux chamber (0.6 to 44 exchanges per minute as compared to 0.167 exchanges per minute).

After leaving the rotameter, the sweep air entered the wind tunnel at one end, passed over the emitting surface, and then exited at the opposite end. At a given sweep air flow rate, a minimum of three volumetric exchanges of sweep air were passed through the wind tunnel prior to VOC sampling. Samples were collected at the lowest flow rate first, moving to the highest flow to minimize potential effects of decreasing VOC concentrations in the emitting source.

Air samples were collected from the air as it exited the middle hole in the Plexiglas top. A fraction of the air exiting the wind tunnel was sampled using stainless steel sorbent tubes (90 mm × 5 mm I.D., SKC, Inc., Eighty-Four, Pa.) filled with either a single-bed 150 mg Tenax TA 60/80 adsorbent or a dual-bed adsorbent consisting of 150 mg Tenax TA 60/80 and 100 mg of Carbopack BAW 6.6% Carbowax 80/120 adsorbent.

Air was pulled through the sorbent tubes at 200 mL min^{-1} using a portable vacuum pump (SKC, Inc., Eighty-Four, Pa.). Sampling time ranged from 5 to 15 min depending on source concentration, with a target sampling volume of 1.0 to 3.0 L per sample. The entire measurement process generally took 90 min or less to collect air samples over three to five velocities on a single source.

Gas Chromatography/Mass Spectrometry

Sorbent tube samples were analyzed by two different methods using a Varian 3800/Saturn 2000 gas chromatograph/mass spectrometer (GC/MS). For method 1, the GC/MS was equipped with a Varian WCOT fused silica, 25 m × 0.25 mm ID, CP-Wax 58 column. Sorbent tube samples were desorbed using a Perkin-Elmer automated thermal desorber (ATD) where the sorbent tube samples were desorbed at 225°C for 15 min, trapped in a quartz cryotrap at -30°C, and then the trap was heated to 225°C and desorbed into the GC/MS. The column oven was ramped from 60°C to 230°C at 6°C min^{-1} for a total run time of 30.3 min.

For method 2, the GC/MS was equipped with an HP-Innowax fused silica, 30 m × 0.25 mm ID column, and sorbent tube samples were desorbed using a Markes Unity automated thermal desorber. The column oven was held at 35°C for 2 min and then ramped from 35°C to 230°C at 6°C min^{-1} for a total run time of 38 min.

All GC/MS samples were analyzed for four sVOCs (phenol, *p*-cresol, indole, and skatole) and seven VFAs (acetic, propionic, isobutyric, butyric, isovaleric, valeric, and hexanoic). In addition to analyzing sorbent tubes with GC/MS, two portable total reduced sulfur (TRS) meters (Jerome 631-X hydrogen sulfide analyzer, Arizona Instrument LLC, Chandler, Ariz.) were also used to measure flux rates of standard solutions of the sulfur-containing VOCs 2-mercaptoethanol and dimethyl sulfide. The TRS meters were factory-calibrated six months prior to their use in this research.

Standards and Method Detection Limits

Standards for the sVOCs were prepared in methanol, and VFA standards were prepared in hexanes. All standards and solvents were FCC kosher grade (>99% purity) purchased from Sigma Aldrich. Standards were prepared using serial dilutions, and then 1 to 10 µL of the standards were injected onto clean tubes using a calibration solution loading rig (CSLR, Markes International). The liquid calibration standard was introduced through the injector septum in argon carrier gas using a standard GC syringe, and then analyzed using the same GC/MS method used for the field samples. For the VFAs, standard curves were made from six standards with one replicate at each concentration. In addition, seven replicates were conducted at two of the concentrations to aid in calculation of method detection limits. For the sVOCs, the standard curves were made from eight standards with seven replicates at each concentration. Standard curves were determined using linear regression with the curve forced to pass through the origin. A typical standard curve for *p*-cresol on sorbent tubes is shown in figure 6. Coefficients of determination (r^2) for the standard curves ranged from 84% to 99% for the seven VFAs and from 92% to 98% for the four sVOCs. Regression slopes and r^2 values for each compound are shown in table 1.

Method detection limits (MDLs) were calculated per U.S. EPA guidelines as the product of the standard deviation of seven replicates and the Student's *t*-value at the 99% confidence level (USEPA, 1999, 1995b). For seven replicates (six degrees of freedom), a *t*-value of 3.14 was used.

The MDL was calculated in mass (ng) and then converted to a reportable MDL in ng L^{-1}. Whenever the calculated MDL was less than the minimum standard for that compound, the minimum standard was reported as the MDL. Method detection limits are presented in table 1.

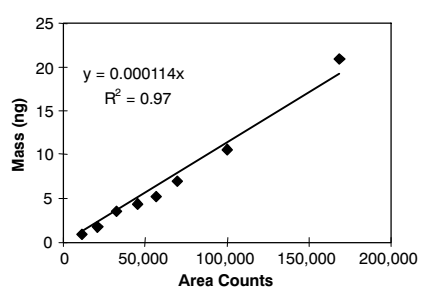

Figure 6. Typical standard curve (*p*-cresol) used for quantification of ambient VOC concentrations. Each point is the average of seven replications.

Table 1. Ranges of mass, method detection limits, and regression coefficients used for the standard curves. For the regression, dependent variable = mass (ng) and independent variable = area counts. MDL = method detection limits.

	Standards, min. to max. (ng)	MDL (ng L^{-1})	Regression Slope	Regression r^2
Acetic acid	1.9 to 75	16.8	7.44E-5	0.97
Propionic acid	1.0 to 40	13.8	1.19E-4	0.85
Butyric acid	2.5 to 100	33.9	7.74E-4	0.90
Isobutyric acid	1.5 to 60	16.2	1.49E-4	0.84
Isovaleric acid	0.06 to 2.5	0.51	3.53E-5	0.99
Valeric acid	0.6 to 25	5.7	8.46E-4	0.97
Hexanoic acid	25 to 1000	564	3.53E-5	0.98
Phenol	1.2 to 30	3.75	1.15E-4	0.98
p-Cresol	0.9 to 21	2.64	1.14E-4	0.97
Indole	0.5 to 12	1.5	2.00E-4	0.92
Skatole	0.25 to 6	0.75	7.85E-5	0.93

Source Samples

Flux rates were measured at varying air flow rates on the following standard solutions and source samples:

1. Standard solutions of acetic acid and phenol each at concentrations of 20 mg L^{-1} and 200 mg L^{-1} in distilled water.
2. Standard solutions of 2-mercaptoethanol (10,000 mg L^{-1}) and dimethyl sulfide (1,000 mg L^{-1}) in distilled water.
3. Evaporation rate of distilled water to determine the gas-film transfer coefficient, k_G^R, for use in the 2-film model and for standardizing the wind tunnel.
4. One composite sample of beef cattle manure from the pen surface of the 600-head beef cattle research feedyard (30% moisture content, wet weight basis).
5. One sample of runoff holding pond effluent from a beef cattle feedyard.
6. Three wastewater samples from dairy lagoons, including one sample from an anaerobic treatment lagoon (dairy lagoon 1) and two samples collected at different times from a secondary storage lagoon (dairy lagoons 2 and 3).

All feedyard and dairy source samples had been collected on earlier research projects and frozen. Source samples were thawed overnight in sealed containers and allowed to reach equilibrium with laboratory room temperature of 21°C to 22°C. The beef runoff pond sample was collected from a 50,000-head commercial beef cattle feedyard. Typical water quality values for runoff collected during the same time period at the same feedyard were pH of 7.7 to 8.0 and EC of 5.3 to 8.0 mmho cm^{-1}. The dairy wastewater samples were collected from a 3,000-head commercial freestall dairy with barn flush and a two-stage anaerobic-aerobic lagoon wastewater system. Typical water quality values from wastewater samples collected during the same time period at the same dairy were: pH 7.6 to 8.0 and EC 6.5 to 10 mmho cm^{-1} (dairy lagoon 1), and pH 8.1 to 8.3 and EC 7.4 to 9.7 mmho cm^{-1} (dairy lagoons 2 and 3). The pH of the distilled water used in the evaporation experiments was 6.65. Additional water quality data from the feedyard and dairy have been previously published (Parker, 2008; Parker et al., 1999; Miller et al., 2001).

Calculation of Flux

Flux density (i.e., emission rate) was calculated as mass per unit area per unit time using equation 12:

$$E_{WT} = \frac{CQ}{A_{WT}} \tag{12}$$

where E_{WT} is the wind tunnel flux rate for the analyte (μg m^{-2} min^{-1}), C is the concentration of component measured in the exit air (μg L^{-1}), Q is the sweep air flow rate (L min^{-1}), and A_{WT} is the surface area enclosed by the wind tunnel (m^2).

Results and Discussion

Effect of Wind Velocity on Flux

Measured Flux from Standard Solutions of Phenol and Acetic Acid

Flux rates vs. air velocity for 20 mg L^{-1} and 200 mg L^{-1} solutions of phenol in water showed strong linear relationships at both concentrations (fig. 7). Similar linear trends were observed for standard solutions of acetic acid in water (data not shown).

Measured Flux from Standard Solutions of 2-Mercaptoethanol and Dimethyl Sulfide

Flux rates vs. air velocity for a 10,000 mg L^{-1} solution of 2-mercaptoethanol and a 1,000 mg L^{-1} solution of dimethyl sulfide are shown in figure 8. The flux for 2-mercaptoethanol was highly dependent on air velocity, while the flux for dimethyl sulfide varied little with air velocity. As shown in figure 2, 2-mercaptoethanol (log H_{cc} ranging from -5.3 to -5.9) falls in the group of VOCs that are gas-film controlled, while dimethyl sulfide (log H_{cc} ranging from -0.3 to -1.2)

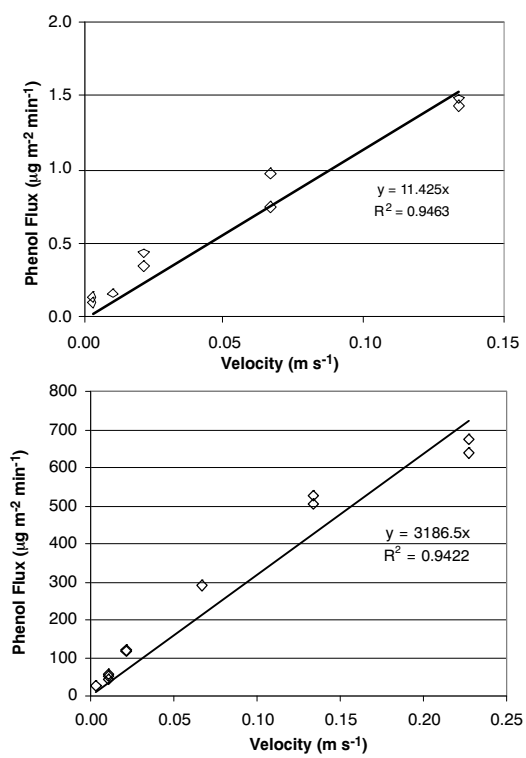

Figure 7. Relationship between measured flux and wind velocity at 2 cm height for standard solutions of phenol in water at 20 mg L^{-1} (top) and 200 mg L^{-1} (bottom).

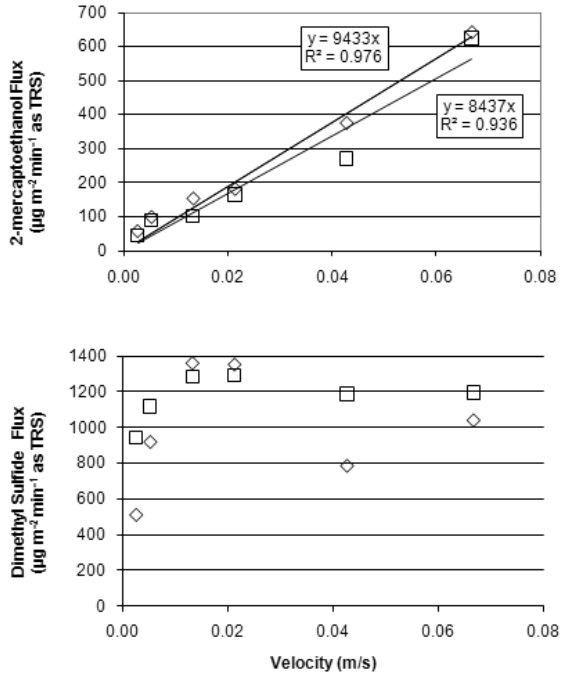

Figure 8. Relationship between measured flux and wind velocity at 2 cm height for standard solutions of 10,000 mg L^{-1} 2-mercaptoethanol in water (top) and 1,000 mg L^{-1} dimethyl sulfide in water (bottom). Squares and diamonds denote measurements by two different portable TRS meters.

falls in the group of VOCs that are liquid-film controlled. The conceptual results of figure 8 are in agreement with the published Henry's law constants of figure 2 and the predicted flux rates of the two-film model with Mills et al. (1985) velocity correction presented in figure 4.

Measured Water Evaporation Rates from the Wind Tunnel

Chao et al. (2005) presented measured k_G^R values for distilled water under various wind speeds measured at a height of 4.5 cm in a wind tunnel (table 2). Using the data of Chao et al. (2005), and a linear relationship for wind speeds between 0 to 0.2 m s^{-1} as measured at 4.5 cm above the water surface, k_G^R and wind speed would be related by the following equation:

$$k_G^R = 157 + 4400\,V \qquad (13)$$

where k_G^R is in m d^{-1}, and V is in m s^{-1}. Chao's values of k_G^R increased 6.6-fold between wind velocities of 0.0 and 0.2 m s^{-1}.

Using the two-film model with Chao's k_G^R values from equation 13, and negating any inhibitive effects from water vapor (i.e., the evaporation rate approaches zero at 100% relative humidity), values of actual evaporation (fig. 9) were

Table 2. Values of Chao et al. (2005) laboratory-derived k_G^R for distilled water under tested wind velocity measured at height of 4.5 cm above water surface.

k_G^R	Wind Velocity (m s^{-1})							
	0	0.2	0.5	0.8	1.0	2.0	4.0	6.0
cm min^{-1}	10.9	72	102	129	143	191	284	359
m d^{-1}	157	1037	1469	1858	2059	2750	4090	5170

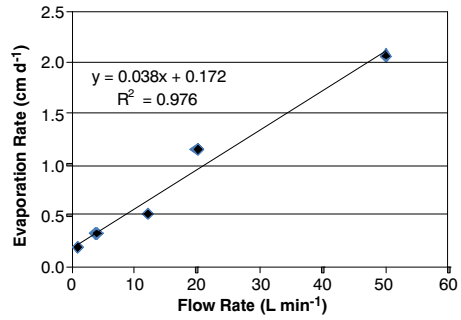

Figure 9. Evaporation rates measured in the wind tunnel at flow rates ranging from 1 L min^{-1} (velocity 0.0027 m s^{-1}) to 50 L min^{-1} (velocity 0.13 m s^{-1}).

plotted against predicted evaporation rates from the wind tunnel (fig. 10). The relative humidity was not measured within the wind tunnel during testing; thus, the effect of water vapor was not included in the model. The relative humidity of the incoming sweep air was consistently 21% throughout the experiments.

As shown in figure 10, the linear approximation for k_G^R between 0 and 0.2 m s^{-1} using equation 13 adapted from Chao et al. (2005) leads to a good approximation of actual evaporation for evaporation rates greater than 4 g m^{-2} min^{-1} (i.e., 0.58 cm d^{-1}), corresponding to wind velocities greater than 0.0388 m s^{-1} and exchange rates greater than 6.3 exchanges per minute.

Given the experimentally measured evaporation rates and negating any effects from water vapor concentrations in the air, the respective k_G^R values as a function of wind speed, which were back-calculated from the two-film model for the wind tunnel used in this research, are presented in table 3. The best fit regression model for the data in table 3 was:

$$k_G^R = -24322\,V^2 + 10039\,V \; (r^2 = 0.981) \qquad (14)$$

where k_G^R is in m d^{-1}, and V is in m s^{-1}.

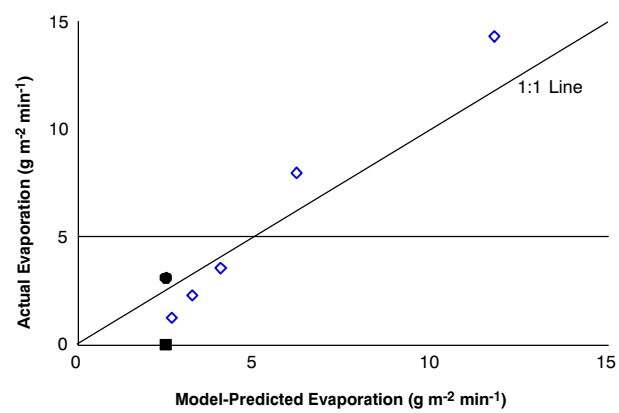

Figure 10. Measured evaporation rates vs. two-film model predicted evaporation rates using the $k_R{}^G$ vs. wind speed of Chao et al. (2005) of equation 13 (shown in diamonds). The solid circle is the measured evaporation rate from an open container in the laboratory (ventilated laboratory with minor air movement), and the solid square is the steady-state evaporation rate of zero for a zero-velocity closed system in the wind tunnel with 100% relative humidity. Note that the model did not account for the inhibition effects from increasing concentrations of water vapor at low velocities (high relative humidity reduces actual evaporation).

Table 3. Experimentally derived values of k_G^R for distilled water under tested wind velocity and exchange rate for the wind tunnel of this research.

		Wind Velocity (m s^{-1})[a]				
Air Exchange Rate (volumes min^{-1})		0.003	0.010	0.032	0.053	0.133
		0.58	2.05	6.31	10.5	26.3
k_G^R	cm min^{-1}	5.5	9.9	15.7	34.7	62.7
	m d^{-1}	79.8	142.0	226.0	500.0	903.0

[a] Average velocity at height of 2.0 cm above water surface.

Our experimentally derived values of k_G^R increased 11.3-fold between wind velocities of 0.00267 and 0.1335 m s^{-1}, a greater increase than reported by Chao et al. (2005). There are three plausible reasons for this increase: (1) our velocities were measured at 2 cm above the surface, whereas Chao's were measured at 4.5 cm above the surface; (2) in Chao's experiments, the relative humidity of the ambient air was 85% to 90%, whereas in our experiments the ambient relative humidity was much lower; and (3) we focused on velocities between 0 and 0.13 m s^{-1}, whereas Chao's experiments ranged from 0 to 6.0 m s^{-1}.

One of the difficulties in comparing emission rates and wind velocity effects is the many different wind tunnel and flux chamber configurations. In a recent review, Hudson and Akoyo (2008b) summarized more than 50 different wind tunnel and flux chamber geometries. Although comparison of emission rates can be difficult among the different wind tunnel and flux chamber devices, the measurement of k_G^R values and distilled water evaporation rates would be useful for standardizing and comparing emission rates from the different devices.

Measured Flux Rates from Samples of Manure/Wastewater

Typical graphs of flux rate vs. air velocity for acetic acid and phenol from three of the manure/wastewater sources are shown in figure 11. Similar trends were observed for all VOCs and all sources, with flux rates increasing with wind velocity. As shown in figure 11, some of the flux-velocity relationships were somewhat curvilinear, whereas others were linear across the entire wind velocity range measured in this research. Rhoades et al. (2005) has shown that an exponential function describes the overall asymptotic nature of gas-phase controlled emissions as a function of air flow rate, where emissions are linear at low air flow rates before eventually approaching zero slope at the maximum emission rate. Because the VOC data were within the linear range of the curve, as evidenced by the high r^2 values, straight lines were fitted to the VOC data using linear regression.

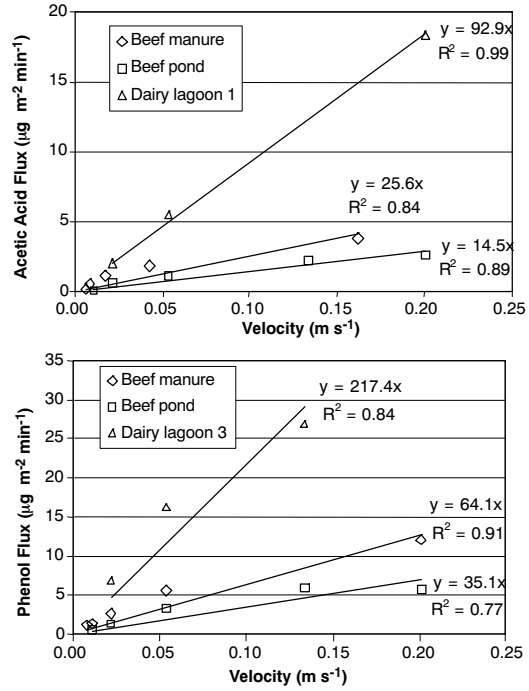

Figure 11. Relationship between measured flux and wind velocity at 2 cm height for acetic acid (top) and phenol (bottom) as measured on three AFO sources. Slopes and corresponding r^2 for these and other samples are summarized in table 4.

A summary of the slopes and coefficients of determination for each of the VOCs and sources is presented in table 4. Most of the r^2 values were greater than 0.90, indicating a strong linear relationship between flux rate and wind velocity, and that greater than 90% of the variability in flux rates could be explained by the varying wind velocities. Large slopes are indicative of higher source concentrations, as the dairy lagoon had considerably higher odor and VOC source concentrations than the beef pond. Minor differences in slope can also be expected for liquid and manure sources, with manure sources often exhibiting a more curvilinear relationship than liquid sources.

Table 4. Values of slope (*m*) and coefficient of determination (r^2) for dependent variable flux rate (µg m^{-2} min^{-1}) vs. independent variable wind velocity (m s^{-1}). All regressions were forced through the origin, giving the model: flux rate = *m* * wind velocity.

	Beef Manure		Beef Runoff Pond		Dairy Lagoon 1		Dairy Lagoon 2		Dairy Lagoon 3	
	m	r^2	*m*	r^2	*m*	r^2	*m*	r^2	*m*	r^2
Acetic	25.6	0.84	14.5	0.89	92.9	0.99	45.1	0.98	63.0	0.99
Propionic	16.3	0.68	6.7	0.63	30.4	0.99	4.89	0.73	7.8	0.97
Isobutyric	7.7	0.92	3.0	0.93	13.2	0.99	8.4	0.98	6.7	0.98
Butyric	341.7	0.92	102.4	0.66	412.6	0.99	31.7	0.04	73.8	0.98
Isovaleric	2.9	0.86	0.8	0.73	3.5	0.91	0.25	0.01	0.64	0.96
Valeric	84.2	0.95	34.0	0.94	131.2	0.96	8.4	0.46	12.0	0.91
Hexanoic	23.8	0.95	21.9	0.95	106.7	0.99	20.4	0.84	25.9	0.73
Phenol	64.1	0.91	35.1	0.77	3152.5	0.36	232.6	0.84	217.4	0.84
p-Cresol	87.3	0.96	12.6	0.93	2918.0	0.79	497.4	0.94	256.5	0.71
Indole	20.1	0.99	3.7	0.95	295.6	0.93	57.0	0.89	18.8	0.71
Skatole	1.0	0.99	0.3	0.99	206.5	0.99	78.6	0.98	63.0	0.99

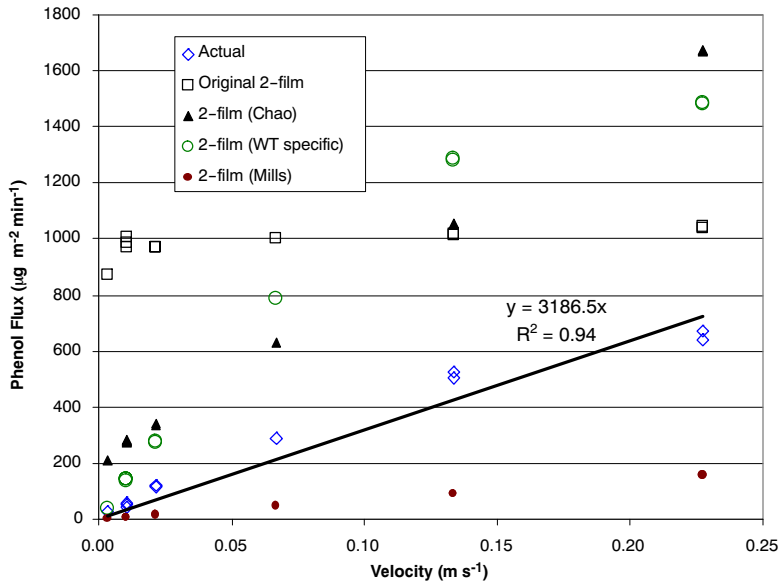

Figure 12. Comparison of actual phenol flux to two-film model predictions using the original two-film model (Whitman, 1923) with velocity corrections of Chao et al. (2005), Mills et al. (1985), and the empirically derived wind-tunnel (WT) specific reference water-vapor gas-film transfer coefficient. All two-film model predictions on this graph were calculated using a Henry's law constant of 2.6E-05.

Comparison of Measured Fluxes to Two-Film Modeled Fluxes

A comparison was made between measured fluxes of phenol (200 mg L^{-1} in water) at differing wind speeds, and fluxes as predicted by the two-film model both with and without various wind velocity corrections (fig. 12). All fluxes were based on the published Henry's law constant of 2.6E-05 for phenol (from Hudson and Ayoka, 2008a). The actual measured flux of phenol is denoted by the open diamonds and straight-line linear regression in figure 12.

The two-film flux with Chao velocity correction was calculated using equations 2, 3, and 5, but using Chao's k_G^R (eq. 13) in equation 6 (denoted by the solid triangles in fig. 12). Although the Chao velocity correction provided a better representation to how actual fluxes increase with velocity, the Chao correction provided flux estimates about 2.5 times the actual flux at the highest velocity.

The two-film flux with wind-tunnel specific k_G^R correction was calculated using equations 2, 3, and 5, but using the wind-tunnel specific k_G^R measured in this research (eq. 14, table 3) (denoted by the open circles in fig. 12). While the specific k_G^R velocity correction provided a better fit near the origin, like Chao's correction it overpredicted the actual phenol flux by about 2.2 times at the highest velocity (fig. 12).

The two-film flux with Mills velocity correction for K_G was calculated using equations 2, 3, 5, and 10 (denoted by the solid circles in fig. 12). Because the Mills velocity correction formula (eq. 10) uses a velocity at 2 m height, the velocity in the wind tunnel at 2 cm height was first converted to the velocity at 2 m height assuming a logarithmic velocity profile with a roughness length of 0.0001 m. The Mills correction underpredicted the actual phenol flux, with a predicted flux about 25% of actual at the highest velocity.

The actual phenol flux was bound on the lower end by the Mills velocity prediction and on the upper end by the Chao velocity prediction (fig. 12).

Given that the two-film model is highly dependent on the Henry's law constant, the Henry's law constant was back-calculated to match the actual phenol flux. The two-film model with the wind-tunnel specific k_G^R correction was found to have the best match with the actual phenol flux using a Henry's law constant of 1.21E-05 at the laboratory temperature of 21.1°C (294.3 K) (fig. 13). This is within the range of published Henry's law constants for phenol (Sander, 1999).

A comparison of the models revealed several important facts. First, a velocity correction is absolutely necessary to accurately represent the effects of wind speed on the flux of compounds with small Henry's law constants, such as phenol. Second, the accuracy of the two-film model is highly dependent on the Henry's law constant. Third, the two-film model with wind-tunnel specific k_G^R and laboratory-determined Henry's law constant can accurately predict actual VOC flux.

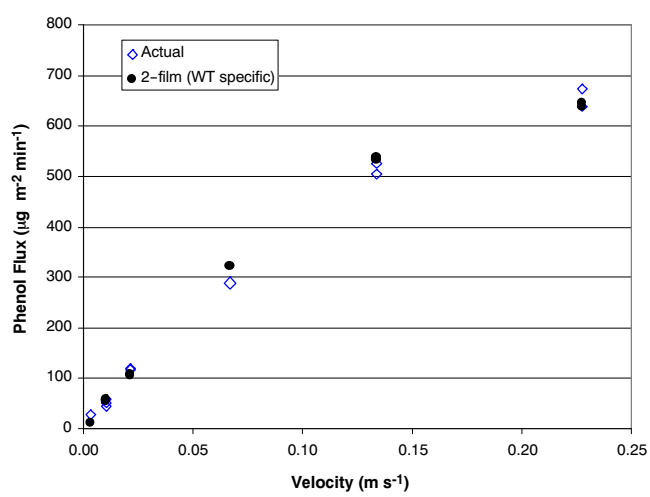

Figure 13. Comparison of actual phenol flux vs. two-film modeled flux using the wind-tunnel specific $k_R{}^G$ and a dimensionless Henry's law constant of 1.21E-05 at 21.1°C.

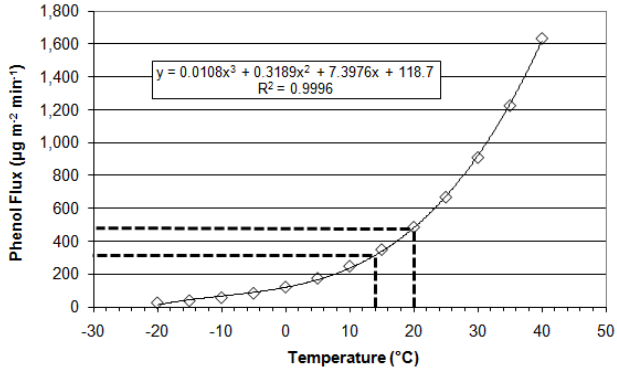

Figure 14. Relationship between temperature and predicted phenol flux using the two-film model at a constant wind tunnel velocity of 0.133 m s^{-1} for a 200 mg L^{-1} phenol in water solution. Dashed lines show the flux adjustment that would be necessary to correct from 20°C to 14°C as discussed in step 3b of the method 3 example.

Temperature Effects on Henry's Law Constants and Two-Film Modeled Fluxes

Sander (1999) presents a range of temperature dependence factors (K, eq. 8) for phenol of 3600 to 7300, with an average of 5,900. Using this average temperature dependence factor, and the laboratory-measured dimensionless Henry's law constant of 1.21E-05 from this research as the baseline H_{cc} at standard conditions for phenol, the resulting plot of how flux varies with temperature at a constant wind tunnel velocity of 0.133 m s^{-1} is shown in figure 14. The slope becomes steeper as temperature increases, indicating that at warmer temperatures, a small change in temperature has a greater effect in magnitude of overall flux.

Wind Tunnel Air Velocity and Temperature Correction Factors to Simulate Actual Field VOC Emissions at AFOs

As demonstrated in this research and by others, wind velocity and temperature have a great impact on emission rates of VOCs found at CAFOs. Thus, correct handling of wind velocity and temperature is critical for estimating accurate and representative field-based emission rates for emission factor calculations. Several methods have been previously proposed for measuring and/or calculating representative field emission rates with wind tunnels:

Method 1

The first and simplest method is to match the wind velocity or air flow rate in the wind tunnel or flux chamber with the expected wind velocities in the field. This method requires a prior knowledge about expected wind velocities at the AFO. Climatological data including average monthly and average annual wind velocities are readily available from weather stations at airports, schools, and governmental research facilities. Wind velocities in the field are typically measured at 2 or 10 m height. Thus, the velocity at the wind tunnel height must be estimated, and the logarithmic velocity profile (Ham, 2005) is often used. This method requires estimation of the roughness length. The logarithmic velocity profile can be calculated such that wind tunnel velocities at a given height can be correlated to equivalent velocities in the field at 2 or 10 m height. To demonstrate how this procedure might be used for the wind tunnel in this research, equivalent

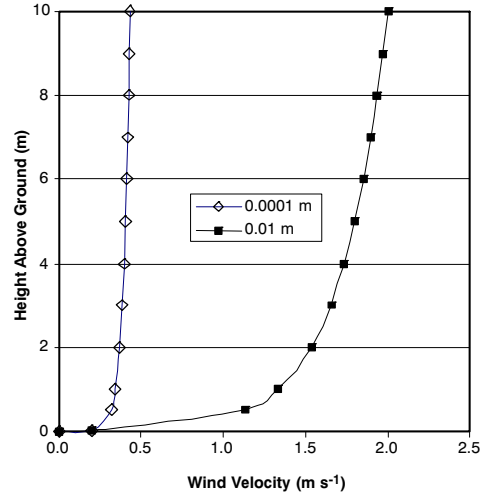

Figure 15. Comparison of logarithmic velocity profiles for surface roughness length (z_0) of 0.0001 m (water) and 0.01 m (manure). Both profiles simulate a wind tunnel velocity of 0.2 m s^{-1} at 2 cm height.

velocities at 2 and 10 m height were calculated using the logarithmic velocity profile (Ham, 2005) for roughness lengths of 0.0001 m for water and 0.01 m for manure (eq. 15):

$$U_2 = U_1 * \ln(z_2/z_0) / \ln(z_1/z_0) \qquad (15)$$

where U_2 is the predicted velocity (m s^{-1}) at height z_2 (m), U_1 is the measured velocity (m s^{-1}) at height z_1 (m), and z_0 is the surface roughness length (m).

Using this method, a wind tunnel velocity of 0.2 m s^{-1} (wind tunnel air flow rate of 75 L min^{-1}) corresponds to velocities at 2 m height of 0.37 and 1.53 m s^{-1} for the water and manure, respectively (fig. 15). Likewise, a wind tunnel velocity of 0.02 m s^{-1} (air flow rate 8 L min^{-1}) corresponds to velocities at 2 m height of 0.037 and 0.15 m s^{-1} for water and manure, respectively. One shortcoming of this method is that it does not account for turbulence, or the combination of both horizontal and vertical wind speeds, within the wind tunnel. Ye et al. (2008) found that turbulence intensity had a great effect on the mass transfer coefficient of ammonia in aqueous solutions. The results of Ye et al. (2008), together with our ongoing research characterizing emissions from various types and designs of wind tunnels and flux chambers, suggests that this first method should be used with caution if used without a detailed characterization of the mass transfer characteristics as a function of wind speed for the wind tunnel or flux chamber used.

Method 2

With the second method, the emission rates are measured using a standard wind velocity or air flow rate, and then the emission rates are corrected (scaled up or down) to match the expected wind velocities in the field. Like method 1, this method requires knowledge about the wind velocity vs. emission rate correlation for the specific wind tunnel or flux chamber, as the specific wind tunnel geometry and air flow rate determine the velocity at a given height above the measuring surface. As demonstrated in this research, most wind velocity vs. emission rate correlations for AFO VOCs are linear within a given wind velocity range. Similar findings have been reported for ammonia (Blanes-Vidal et al., 2007; Rhoades et al., 2005) and odor/VOCs (Hudson and Ayoko, 2009). Thus, within this range, the linear relationship

can be used to scale the field-measured emission rates to an average emission rate for a given time period.

Method 3

The third method follows the logic first proposed by Vlek and Stumpe (1978), who compared evaporation and ammonia emissions from small containers (120 × 120 × 150 mm) placed outdoors to evaporation and ammonia emissions measured in the laboratory. It would be difficult and cumbersome to quantify volatilization of VOCs in small containers in the field. However, because the volatilization of AFO VOCs is correlated to evaporation (as demonstrated by similar Henry's constants in fig. 2, and through the wind-tunnel specific reference gas-film transfer coefficient for water vapor, k_G^R demonstrated in fig. 13), the Class A pan evaporation data could be used for correcting previously measured field-based wind tunnel emissions. This method requires knowing the evaporation vs. wind speed and temperature relationship for the specific wind tunnel or flux chamber being used. As mentioned earlier, emission rates are not just a function of horizontal wind velocity, but also of turbulence, which is a measure of both horizontal and vertical wind velocity (Ye et al., 2008). Laboratory testing of wind tunnel evaporation as a function of wind speed provides a direct measure of emissions as affected by both wind velocity and turbulence. A step-by-step example of how the local pan evaporation data could be used to correct for average annual wind speed and temperature is as follows:

Step 1. The average annual Class A pan evaporation rate and temperature for the AFO site is determined from historic weather records, for example, 0.71 cm d^{-1} and 14.0°C for Amarillo, Texas (WRCC, 2005).

Step 2. The wind velocity in the wind tunnel that gives this evaporation rate at the given average annual temperature is determined in the laboratory. For the wind tunnel used in this research, a sweep air flow rate of 25 L min^{-1} (wind velocity of 0.067 m s^{-1}) is required at the average annual temperature of 14°C to obtain an evaporation rate of 0.71 cm d^{-1} (fig. 16). Figure 16 was constructed by combining the data from figure 9 with the two-film model predicted evaporation rates using the wind-tunnel specific reference gas-film transfer coefficient and the predicted temperature vs. evaporation relationship similar to the one shown in figure 14.

Step 3a. The emission rate measured in the field is corrected first for ambient temperature with two options available at this point. Suppose the ambient temperature at the time of sampling was 20°C, then the wind tunnel flow rate could be set at 16 L min^{-1} using figure 16. However, if the ambient temperature is unknown at the time of sampling (for example, if data are being recorded at a nearby weather station), then a flow rate must be selected for field measurements, making post-sampling wind speed and temperature corrections necessary as outlined in step 3b.

Step 3b. For this example, suppose the ambient temperature was 20°C at the time of sampling, and a flow rate of 20 L min^{-1} (0.053 m s^{-1}) was actually used in the field sampling. Two correction factors would be needed: a temperature correction factor and a wind speed correction factor. A temperature correction factor of 0.65 would first be applied to the measured emission rate (ratio = 314/481, from fig. 14) to adjust 20°C to the average annual temperature of 14°C. Because the relationship between temperature and emission rate is approximately linear in the range between

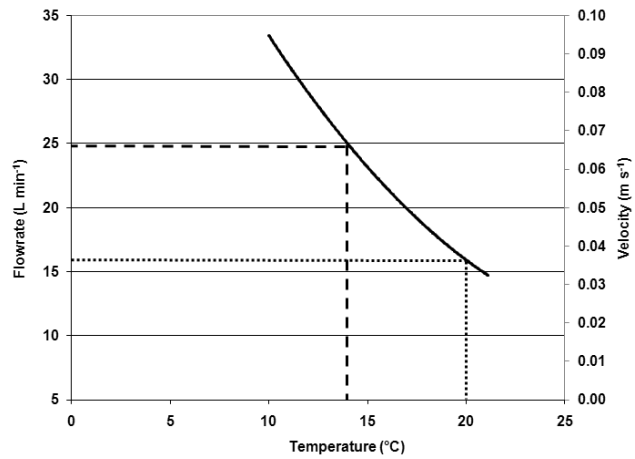

Figure 16. Required sweep air flow rate and corresponding wind velocity to obtain the average annual pan evaporation rate of 0.71 cm d^{-1} for Amarillo, Texas, at various temperatures for the wind tunnel of this research. A flow rate of 25 L min^{-1} is required at the average annual temperature of 14°C (heavy dashed line).

14°C and 20°C, the ratio of 0.70 (i.e., 14/20) could also be used to approximate the temperature correction factor. That leaves only the wind speed correction factor. At the average annual temperature of 14°C, a flow rate of 25 L min^{-1} (0.067 m s^{-1}) is required to simulate 0.71 cm d^{-1} evaporation (fig. 16). Because 20 L min^{-1} (0.053 m s^{-1}) is less than 25 L min^{-1} (0.067 m s^{-1}), the wind speed correction factor would be greater than 1.0. In this case, the correction factor can be obtained knowing that evaporation is linearly correlated with the air speeds investigated in this research, so the wind velocity correction factor would be 1.25 (i.e., 25/20). The combined temperature-wind speed correction would be obtained by multiplying the two correction factors together (0.65 × 1.25 = 0.81). Thus, for this example, the emission rate measured at 20°C and 20 L min^{-1} would be corrected to average annual weather conditions by multiplying by 0.81.

Although air velocity and temperature are the primary factors affecting emissions of VOC, other factors such as pH and moisture content can also affect emission rates of VOC, VFA, H_2S, TRS, CO_2, NH_3, and odor (Canh et al., 1998; Cole et al., 2008; Parker et al., 2005). For example, high pH favors NH_3 emissions, while low pH favors VFA and H_2S emissions (Arogo et al., 1999; Le et al., 2005). Researchers developing process-based models for emissions from animal feeding operations should account for all important variables.

Current and ongoing research conducted by the authors will focus on correction factors for a variety of wind tunnels and flux chambers commonly used to measure VOC and ammonia emissions from animal feeding operations. A summary of that research can be found in Parker et al. (2009) and Paris et al. (2009). Simultaneous flux measurements with a variety of flux chambers and wind tunnels will allow for correction factors for a variety of measurement devices.

Conclusions

The following conclusions were drawn from this research:

- The emission rates of eleven VOCs found at AFOs increased linearly between volumetric air exchange rates of 0.6 to 39 exchanges per minute (corresponding to calculated average longitudinal air velocities of

0.003 to 0.2 m s^{-1}). These results show that wind velocity greatly affects VOC emissions from AFOs. For this reason, wind velocity effects should be included in emission factor estimations for these VOCs.

- The two-film models with different wind speed corrections predicted widely varying fluxes. As shown by the two-film models and Henry's law constants, VOCs found at AFOs behave differently than those found at most industrial and hazardous waste sites. Emissions of VOCs found at AFOs are greatly affected by wind velocity, as opposed to most industrial-type and hazardous waste VOC emissions, which are affected little by wind velocity. The two-film model with an experimentally derived reference gas-film transfer coefficient was found to reliably predict VOC flux at velocities between 0.003 and 0.23 m s^{-1}. However, the two-film model did not reliably predict VOC flux with other wind velocity correction formulae, an indication that flux is a function of wind tunnel geometry and not just wind velocity or sweep air flow rate.
- As demonstrated in this article, water evaporation would be useful not only for standardizing and comparing emission rates from wind tunnels and flux chambers, but also in correcting for atmospheric conditions in the field. Correction factors for wind speed and temperature are demonstrated in this article. Because correction factors are dependent on the geometry of the wind tunnel or flux chamber, a generic wind speed or temperature correction factor cannot be presented at this time.

Acknowledgements

This research was a collaborative project supported by USDA-CSREES Project No. TS-2006-06009 entitled "Air Quality: Odor, Dust, and Gaseous Emissions from Concentrated Animal Feeding Operations in the Southern Great Plains."

References

Aquino, F. L., S. C. Capareda, C. B. Parnell, S. Mukhtar, R. Lacey, and B. Shaw. 2007. Comparison of partial reactive organic gases (ROG) emission factors from a dairy and beef feedlot. ASABE Paper No. 074006. St. Joseph, Mich.: ASABE.

Arogo, J., R. H. Zhang, G. L. Riskowski, and D. L. Day. 1999. Mass transfer coefficient for hydrogen sulfide emission from aqueous solutions and liquid swine manure. *Trans ASAE* 42(5): 1455-1462.

Bianchi, A. P., and M. S. Varney. 1997. Volatilisation processes in wastewater treatment plants as a source of potential exposure to VOCs. *Ann. Occup. Hyg.* 41(4): 437-454.

Bidleman, T. F., and L. L. McConnell. 1995. A review of field experiments to determine air-water gas exchange of persistent organic pollutants. *Sci. Total Environ.* 159(2-3): 101-117.

Blanes-Vidal, V., M. N. Hansen, S. Pedersen, and H. B. Rom. 2007. Emissions of ammonia, methane, and nitrous oxide from pig houses and slurry: Effects of rooting material, animal activity, and ventilation rate. *Agric. Ecosys. and Environ.* 124(3): 237-244.

Buonicore, A. J., and W. Davis. 1992. *Air Pollution Engineering Manual.* New York, N.Y.: Air and Waste Management Association.

Canh, T. T., A. J. A. Aarnink, M. W. A. Verstegen, and J. W. Schrama. 1998. Influence of dietary factors on the pH and ammonia emission of slurry from growing-finishing pigs. *J. Animal Sci.* 76(4): 1123-1130.

Carter, W. P. L. 1994. Development of ozone reactivity scales for volatile organic compounds. *J. Air Waste Mgmt. Assoc.* 44: 881-899.

Chao, H.-P., J.-F. Lee, C.-K. Lee, and H.-C. Huang. 2005. An alternative method for predicting organic solute volatilization rates under gas and liquid turbulence. *Chemosphere* 59(5): 711-720.

Cole, N. A., R. W. Todd, D. B. Parker, and M. B. Rhoades. 2007. Challenges in using flux chambers to measure ammonia emissions from simulated feedlot pen surfaces and retention ponds. In *Proc. Intl. Symposium on Air Quality and Waste Management for Agriculture.* St. Joseph, Mich.: ASABE.

Cole, N. A., R. Todd, B. Auvermann, and D. Parker. 2008. Auditing and assessing air quality in concentrated feeding operations. *Prof. Animal Scientist* 24(1): 1-22.

Delos, C. G., W. L. Richardson, J. V. DePinto, R. Ambrose, P. Rodgers, K. Rygwelski, J. St. John, W. Shaughnessy, T. Fana, and W. Christie. 1984. Technical guidance manual for performing waste load allocations: Chapter 3. Toxic substances: In *Book II: Streams and Rivers*. EPA-440/4-84-022. Washington, D.C.: U.S. Environmental Protection Agency.

Eklund, B. 1992. Practical guidance for flux chamber measurements of fugitive volatile organic emission rates. *J. Air Waste Mgmt. Assoc.* 42(12): 1583-1591.

Filipy, J., B. Rumburg, G. Mount, H. Westbery, and B. Lamb. 2006. Identification and quantification of volatile organic compounds from a dairy. *Atmos. Environ.* 40(8): 1480-1494.

Fowler, D., M. Coyle, C. Flechard, K. Hargreaves, E. Nemitz, R. Storeton-West, M. Sutton, and J.-W. Erisman. 2001. Advances in micrometeorological methods for the measurement and interpretation of gas and particle nitrogen fluxes. *Plant and Soil* 228(1): 117-129.

Gholson, A., J. Albritton, and R. Jayanty. 1989. Evaluation of the flux chamber method for measuring volatile organic emissions from surface impoundments. EPA/600/3-89/008. Research Triangle Park, N.C.: U.S. Environmental Protection Agency.

Gholson, A. R., J. R. Albritton, and R. K. M. Jayanty. 1991. Evaluation of an enclosure method for measuring emissions of volatile organic compounds from quiescent liquid surfaces. *Environ. Sci. Tech.* 25(3): 519-524.

Ham, J. M. 2005. Useful equations and tables in micrometeorology. In *Micrometeorology in Agricultural Systems*, 533-599. J. L. Hatfield, and J. M. Baker, eds. Agronomy Monograph No. 17. Madison, Wisc.: American Society of Agronomy.

Hudson, N. A. 2009. Investigation of mechanisms governing emission of odorants, Chapter 7. PhD diss. Brisbane, Queensland, Australia: Queensland University of Technology.

Hudson, N., and G. A. Ayoko. 2008a. Odour sampling 1: Physical chemistry considerations. *Bioresource Tech.* 99(10): 3988-3992.

Hudson, N., and G. A. Ayoko. 2008b. Odour sampling 2: Comparison of physical and aerodynamic characteristics of sampling devices: A review. *Bioresource Tech.* 99(10): 3993-4007.

Hudson, N., and G. A. Ayoko. 2009. Comparison of emission rate values for odour and odorous chemicals derived from two sampling devices. *Atmos. Environ.* 43(20): 3175-3181.

Hudson, N., G. A. Ayoko, M. Dunlop, D. Duperouzel, D. Burrell, K. Bell, E. Gallagher, P. Nicholas, and N. Heinrich. 2009. Comparison of odour emission rates measured from various sources using two sampling devices. *Bioresource Tech.* 100(1): 118-124.

IUCLID5. 2007. Substance: 2-mercaptoethanol. Paris, France: OECD, International uniform chemical information database. Available at: www.oecd.org/dataoecd/41/7/39227240.pdf. Accessed 28 May 2008.

Kienbusch, M. R. 1986. Measurement of gaseous emission rates from land surfaces using an emission isolation flux chamber: User's guide. EPA-600/8-86/008. Washington, D.C.: U.S. Environmental Protection Agency.

Kim, K., S. O. Baek, Y. Choi, Y. Sunwoo, E. Jeon, and J. H. Hong. 2006. The emissions of major aromatic VOC as landfill gas from urban landfill sites in Korea. *Environ. Monit. and Assess.* 118(1-3): 407-422.

Kissel, D. E., H. L. Brewer, and G. F. Arkin. 1977. Design and test of a field sampler for ammonia volatilization. *SSSA J.* 41(6): 1133-1138.

Le, P. D., A. J. A. Aarnink, N. W. M. Ogink, and M. W. A. Verstegen. 2005. Effects of environmental factors on odor emission from pig manure. *Trans. ASABE* 48(2): 757-765.

Lee, J.-F., H.-P. Chao, C. T. Chiou, and M. Manes. 2004. Turbulence effects on volatilization rates of liquids and solutes. *Environ. Sci. Tech.* 38(16): 4327-4333.

Lewis, W., and W. Whitman. 1924. Principles of gas adsorption. *J. Ind. and Eng. Chem.* 16: 1215-1220.

Leyris, C., J.-M. Guillot, J.-L. Fanlo, and L. Pourtier. 2005. Comparison and development of dynamic flux chambers to determine odorous compound emission rates from area sources. *Chemosphere* 59(3): 415-421.

Lindberg, S. E., H. Zhang, A. F. Vette, M. S. Gustin., M. O. Barnett, and T. Kuiken. 2002. Dynamic flux chamber measurement of gaseous mercury emission fluxes over soils: Part 2. Effect of flushing flow rate and verification of a two-resistance exchange interface simulation model. *Atmos. Environ.* 36(5): 847-859.

Liss, P. S., and P. G. Slater. 1974. Flux of gases across the air-sea interface. *Nature* 247(5438): 181-184.

Mackie, R. I., P. G. Stroot, and V. H. Varel. 1998. Biochemical identification and biological origin of key odor components in livestock waste. *J. Animal Sci.* 76(5): 1331-1342.

Mata-Alvarez, J., S. Mace, and P. Llabres. 2000. Anaerobic digestion of organic solid wastes: An overview of research achievements and perspectives. *Bioresource Tech.* 74(1): 3-16.

Meisinger, J. J., A. M. Lefcourt, and R. B. Thompson. 2001. Construction and validation of small mobile wind tunnels for studying ammonia volatilization. *Applied Eng. in Agric.* 17(3): 375-381.

Miller, B. L., D. B. Parker, J. M. Sweeten, and C. Robinson. 2001. Response of seven crops and two soils to application of beef cattle feedyard effluent. *Trans. ASAE* 44(2): 309-315.

Mills, W. B., D. B. Porcella, M. J. Ungs, S. A. Gherini, K. V. Summers, L. Mok, G. L. Rupp, G. L. Bowie, and D. A. Haith. 1985. Water quality assessment: A screening procedure for toxic and conventional pollutants in surface and ground water (revised 1985): Part 1. EPA-600/6-85-002a. Athens, Ga.: U.S. EPA Environmental Research Laboratory.

NAS. 2003. Air emissions from animal feeding operations: Current knowledge, future needs. Washington, D.C.: National Research Council.

Paris, C. S., D. B. Parker, N. A. Cole, R. W. Todd, E. A. Caraway, M. B. Rhoades, B. Baniya and T. B. Brown. 2009. Comparison of ammonia emissions determined with different sampling methods. In *Proc. Texas Animal Manure Management Issues (TAMMI) Conf.*, 83-90. College Station, Tex.: Texas A&M University.

Parker, D. B. 2008. Reduction of odor and VOC emissions from a dairy lagoon. *Applied Eng. in Agric.* 24(5): 647-655.

Parker, D. B., B. W. Auvermann, and D. L. Williams. 1999. Comparison of evaporation rates from feedyard pond effluent and clear water as applied to seepage predictions. *Trans. ASAE* 42(4): 981-986.

Parker, D. B., M. B. Rhoades, G. L. Schuster, J. A. Koziel, and Z. L. Perschbacher. 2005. Odor characterization at open-lot beef cattle feedyards using triangular forced-choice olfactometry. *Trans. ASAE* 48(4): 1527-1535.

Parker, D. B., Z. Buser, E. Caraway, M. Rhoades, M. Olsen, K. Casey, J. Spears, and G. Green. 2007. VOC concentrations downwind of beef feedlots during intense odour events. In *Proc. 14th IUAPPA World Congress.* Olinda, Victoria, Australia: Clean Air Society of Australia and New Zealand.

Parker, D. B., N. A. Cole, K. D. Casey, G. Galvin, R. Ormerod, C. S. Paris, E. A. Caraway, and M. B. Rhoades. 2009. Wind tunnels vs. flux chambers: Area source emission measurements and the necessity for VOC and odour correction factors. In *Proc. 19th Intl. Clean Air and Environment (CASANZ) Conf.* Olinda, Victoria, Australia: Clean Air Society of Australia and New Zealand.

Rabaud, N. E., S. E. Ebeler, L. L. Ashbaugh, and R. G. Flocchini. 2002. The application of thermal desorption GC/MS with simultaneous olfactory evaluation for the characterization and quantification of odor compounds from a dairy. *J. Agric. Food Chem.* 50(18): 5139-5145.

Rabaud, N. E., S. E. Ebeler, L. L. Ashbaugh, and R. G. Flocchini. 2003. Characterization and quantification of odorous and non-odorous volatile organic compounds near a commercial dairy in California. *Atmos. Environ.* 37(7): 933-940.

Rhoades, M. B., D. B. Parker, N. A. Cole, R. DeOtte, B. W. Auvermann, and Z. L. Perschbacher-Buser. 2005. Factors affecting ammonia emission measurements with surface isolation flux chambers. ASABE Paper No. 054026. St. Joseph, Mich. ASABE.

Ryden, J. C., and D. Lockyer. 1985. Evaluation of a system of wind tunnels for field studies of ammonia loss from grassland through volatilisation. *J. Sci. Food Agric.* 36(9): 781-788.

Sadek, S. E., J. D. Smith, A. T. Watkin, and R. Gebel. 1996. Mass transfer of volatile organics from large open basins. *Environ. Prog.* 15(2): 82-92.

Sander, R. 1999. Compilation of Henry's law constants for inorganic and organic species of potential importance in environmental chemistry. Version 3. Mainz, Germany: Max-Planck Institute for Chemistry. Available at: www.mpch-mainz.mpg.de/~sander/res/henryhtml.

Sawyer, C. N., and P. L. McCarty. 1978. *Chemistry for Environmental Engineering*. 3rd ed. New York, N.Y.: McGraw-Hill.

Schwarzenbach, R. P., P. M. Gschwend, and D. M. Imboden. 2003. *Environmental Organic Chemistry.* 2nd ed. Hoboken, N.J.: Wiley-Interscience.

Sunesson, A.-L., J. Gullberg, and G. Blomquist. 2001. Airborne chemical compounds on dairy farms. *J. Environ. Monit.* 3(2): 210-216.

USEPA. 1982. Volatilization of organic pollutants from water. EPA-600/3-82-019. Athens, Ga.: U.S. Environmental Protection Agency.

USEPA. 1995a. Air quality: Revision to definition of volatile organic compounds - Exclusion of acetone. 40 CFR 51.100(s). Washington, D.C.: U.S. Environmental Protection Agency. Available at: www.epa.gov/EPA-AIR/1995/June/Day-16/pr-752.html.

USEPA. 1995b. Definition and procedure for the determination of the method detection limit - Revision 1.11. 40 CFR Part 136, Appendix B. Washington, D.C.: U.S. Environmental Protection Agency.

USEPA. 1999. Determination of volatile organic compounds in ambient air using active sampling onto sorbent tubes. Compendium method TO-17. Cincinnati, Ohio: U.S. Environmental Protection Agency.

Vlek, P. L. G., and J. M. Stumpe. 1978. Effects of solution chemistry and environmental conditions on ammonia volatilization losses from aqueous systems. *SSSA J.* 42(3): 416-421.

Wanninkhof, R. 1992. Relationship between wind speed and gas exchange over the ocean. *J. Geophysical Res.* 97(C5): 7373-7382.

Watkins, S. H., R. F. Strand, D. S. Debell, and J. Esch, Jr. 1972. Factors influencing ammonia losses from urea applied to northwestern forest soils. *SSSA Proc.* 36(2): 354-357.

Whitehead, D. C., and N. Raistrick. 1991. Effects of some environmental factors on ammonia volatilization from simulated livestock urine applied to soil. *Biol. Fert. Soils* 11(4): 279-284.

Whitman, W. G. 1923. The two-film theory of gas absorption. *Chem. and Metallurgical Eng.* 29: 146-148.

WRCC. 2005. Texas monthly average temperatures. Reno, Nev.: Western Regional Climate Center, Desert Research Institute. Available at: www.wrcc.dri.edu/htmlfiles/tx/tx.avg.html.

Wright, D. W., D. K. Eaton, L. T. Nielsen, F. W. Kuhrt, J. A. Koziel, J. P. Spinhirne, and D. B. Parker. 2005. Multidimensional gas chromatography-olfactometry for identification and prioritization of malodors from confined animal feeding operations. *J. Agric. Food Chem.* 53(22): 8663-8672.

Ye, Z., G. Zhang, B. Li, J. S. Strom, G. Tong, and P. J. Dahl. 2008. Influence of airflow and liquid properties on the mass transfer coefficient of ammonia in aqueous solutions. *Biosystems Eng.* 100(3): 422-434.

Zahn, J. A., J. L. Hatfield, Y. S. Do, A. A. DiSpirito, D. A. Laird, and R. L. Pfeiffer. 1997. Characterization of volatile organic emissions and wastes from a swine production facility. *J. Environ. Qual.* 26(6): 1687-1696.

Zhang, H., S. E. Lindberg, M. O. Barnett, A. F. Vette, and M. S. Gustin. 2002. Dynamic flux chamber measurement of gaseous mercury emission fluxes over soils: Part 1. Simulation of gaseous mercury emissions from soils using a two-resistance exchange interface model. *Atmos. Environ.* 36(5): 835-846.